Optical echo spectroscopy and phase relaxation of Nd^{3+} ions in CaF_2 crystals

T. T. Basiev, A. Ya. Karasik, and V. V. Fedorov

Institute of General Physics, Russian Academy of Sciences, 117942 Moscow, Russia

K. W. Ver Steeg

Microelectronics Research Center, Iowa State University, Ames, Iowa 50011, U.S.A.
(Submitted 18 June 1997)
Zh. Éksp. Teor. Fiz. **113**, 278–290 (January 1998)

Accumulated photon echoes have been used to investigate the mechanisms of optical dephasing in CaF_2 crystals activated by Nd^{3+} ions. Tunable picosecond laser radiation, which permits the selective excitation of various Nd^{3+} optical centers in the $^4I_{9/2}\rightarrow{}^4G_{5/2},{}^2G_{7/2}$ transition, is used. The optical phase relaxation times measured at temperatures from 9 to 50 K permit determination of the homogeneous widths of the transitions between the low-lying $^4I_{9/2}$ Stark level and three excited $^4G_{5/2},{}^2G_{7/2}$ levels, and calculation of the constants of the inter-Stark relaxation transitions in the ground and excited multiplets for the rhombic *N* and *M* Nd^{3+} centers in CaF_2 crystals. An analysis of the temperature dependence of the homogeneous linewidth of the transitions between low-lying Stark levels of the ground and excited states shows that the mechanism of optical dephasing in the crystals investigated is described well by direct relaxation processes with resonant inter-Stark absorption of one phonon in the ground and excited states. At $T=9$ K, the homogeneous linewidth Γ_h in CaF_2 crystals is almost an order of magnitude smaller than Γ_h in disordered CaF_2–YF_3 crystals. This difference can be attributed to the significantly greater spectral phonon density of states in disordered crystals.
 [S1063-7761(98)01901-5]

1. INTRODUCTION

The investigation of fundamental optical dephasing processes in organic and inorganic glasses and crystals activated by trivalent rare-earth ions has been the subject of numerous investigations,[1,2] since understanding the relaxation processes of excited states of impurity ions in a solid is not only a very important scientific problem, but also a necessary condition for creating efficient solid-state lasers. In the present work the optical phase relaxation of Nd^{3+} ions in CaF_2 crystals was investigated using accumulated photon echoes.[3,4]

The structure of the optical Nd^{3+} centers in CaF_2 crystals was fully investigated in earlier studies. In Refs. 5–7 the concentration method and selective laser excitation were successfully employed to elucidate the composition of the Nd^{3+} centers in CaF_2 and to determine the positions of the Stark sublevels for each type of center. In Refs. 8 and 9 the symmetry of the principal Nd^{3+} centers in CaF_2 crystals was investigated using ESR.

Accumulated photon echoes permit direct measurement of the phase relaxation kinetics and determination of the homogeneous linewidth Γ_h of a transition, which is not distorted by the inhomogeneous broadening of the spectra Γ_{ih}. In the present work we investigate the temperature dependence of the homogeneous linewidth of the $^4I_{9/2}\rightarrow{}^4G_{5/2},{}^2G_{7/2}$ transition in the dimeric and trimeric Nd^{3+} cluster centers in the temperature range 9–50 K. The experimental plot of $\Gamma_h(T)$ can be described within terms of direct relaxation transitions between Stark sublevels of the ground and excited states, with the absorption and emission of one phonon.

2. INHOMOGENEOUS SPLITTING AND BROADENING OF THE ABSORPTION LINES OF Nd^{3+} IN CaF_2 CRYSTALS

The CaF_2:Nd^{3+} crystals were grown by a modified Bridgeman method in a metered fluorine atmosphere in the absence of oxygen-bearing compounds.[5] The concentration of NdF_3 was varied from 0.1 to 7 wt. %. In the cubic fluorite structure Nd^{3+} ions can be distributed among sites of differing structure, which have different spectra.[5–7] According to Ref. 7, triply charged Nd^{3+} ions replace doubly charged Ca^{2+} ions during growth in a fluorinating atmosphere, and the crystal is saturated by interstitial fluorine ions to maintain electroneutrality. At very low Nd^{3+} concentrations, the charge compensation can be nonlocal (it can be effected by distant interstitial F_i^- ions) and can leave the original cubic symmetry of the ligand field around each Nd^{3+} ion unchanged. As the concentration of impurity Nd^{3+} ions and, therefore, of the F_i^- ions compensating them rises, they are attracted to one another to form dipoles, and the symmetry of the local environment of each Nd^{3+} ion changes from cubic to tetragonal (an *L* center forms, in which the F_i^- ion occupies a nearby interstitial site[7]). As the concentration is further increased, the mutual attraction of the Nd^{3+}–F_i^- dipoles leads to the formation of dimeric $(Nd^{3+}–F_i^-)_2$ clusters or *M* centers and tetrameric $(Nd^{3+}–F_i^-)_4$ clusters or *N* centers with rhombic symmetry. In these clusters two (or four) Nd^{3+} ions replace two (or four) Ca^{2+} ions. In this case two or four fluorine ions occupy nearby free interstitial sites to achieve local charge compensation.

The relative concentration of particular optical centers in CaF_2:Nd^{3+} crystals depends primarily on the total concen-

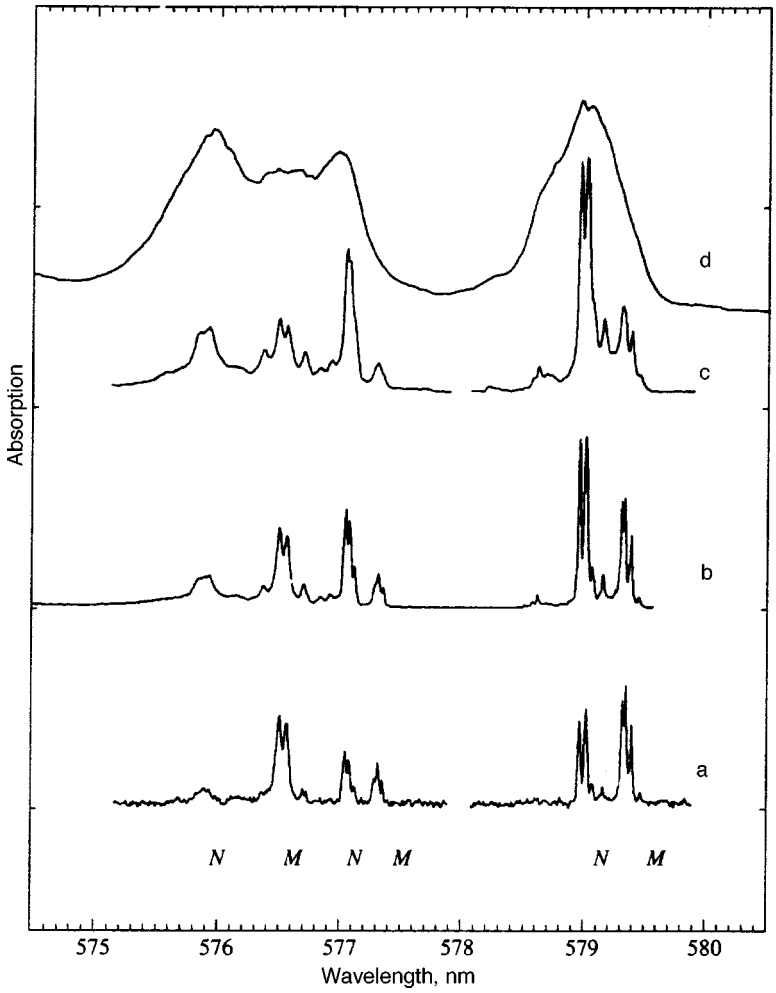

FIG. 1. Absorption spectra of the M and N Nd^{3+} centers in CaF_2 crystals in the $^4I_{9/2}\rightarrow{}^4G_{5/2},{}^2G_{7/2}$ transition at $T=9$ K for various concentrations of NdF_3, wt. %: a) 0.1, b) 0.3, c) 1, d) 7.

tration of NdF_3 introduced into the CaF_2 crystal during its synthesis. Figure 1 presents the absorption spectra of neodymium ions between the low-lying Stark sublevels of the $^4I_{9/2}\rightarrow{}^4G_{5/2},{}^2G_{7/2}$ transition in a CaF_2 crystal at $T=9$ K. According to Refs. 5–7, absorption at these wavelengths corresponds to a transition between the ground $^4I_{9/2}$ level and the first three Stark sublevels of the $^4G_{5/2},{}^2G_{7/2}$ multiplets of the M and N centers. It is clear from the figure that the absorption associated with M centers dominates at an NdF_3 concentration equal to 0.1%. Increasing the NdF_3 concentration from 0.1 to 1.0 wt. % results in an increase in the concentration of the tetrameric N centers in comparison with the dimeric M centers.[7] When the NdF_3 concentration is increased significantly (to more than 1 wt. %), the system should be treated as a crystalline solid solution. In this case NdF_3 is regarded not as an impurity, but as one of the components of the solid solution.

Solid solutions are characterized by statistical disorder, under which it becomes difficult to speak about order in distant coordination spheres. A significant increase in the concentration of NdF_3 to 7 wt. % is manifested by an increase in the number of centers, and passage from inhomogeneous line splitting to inhomogeneous broadening of the spectra (Fig. 1, curve d), where weakly structured broad bands appear instead of sets of narrow lines. In this case, the concentrations of the various components of the solid solution are already comparable, and the M and N cluster centers enlarge, possibly forming tetrameric, pentameric, and more aggregated clusters. The symmetry of the new clusters can be lower than that of the M and N cluster centers, and the statistics of the Nd^{3+} states in crystal fields of different symmetry and strength lead to considerable inhomogeneous broadening of the lines (comparable to glasses), amounting ~ 30 cm^{-1} (Fig. 1, curve d).

Figure 2 presents the absorption spectra of the CaF_2:Nd^{3+} crystals investigated in the $^4I_{9/2}\rightarrow{}^4G_{5/2},{}^2G_{7/2}$ transition between the low-lying Stark levels as the NdF_3 concentration is varied from 0.1 to 1 wt. % at $T=9$ K, which were recorded with a resolution of 0.22 cm^{-1}. As seen from the figure, the absorption spectra consist of two groups of lines with $\lambda=579.4$ and 579.0 nm. The minimum values of the linewidth in Fig. 2 are determined by the spectral resolution. It can be seen from the figure that varying the NdF_3 concentration from 0.1 to 1 wt. % results in variation of the specific concentrations of the M and N centers toward the more aggregated N centers, while the relative splitting of the absorption coefficients within each group of lines remains constant. In the figure, each of these groups corresponds to four lines with splitting for the M centers ranging from 0.9 to 4.3 cm^{-1} (between the outermost lines) and splitting for the N centers ranging from ~ 1.8 to 6 cm^{-1}. The lack of similar splitting in the absorption spectra in other transitions sug-

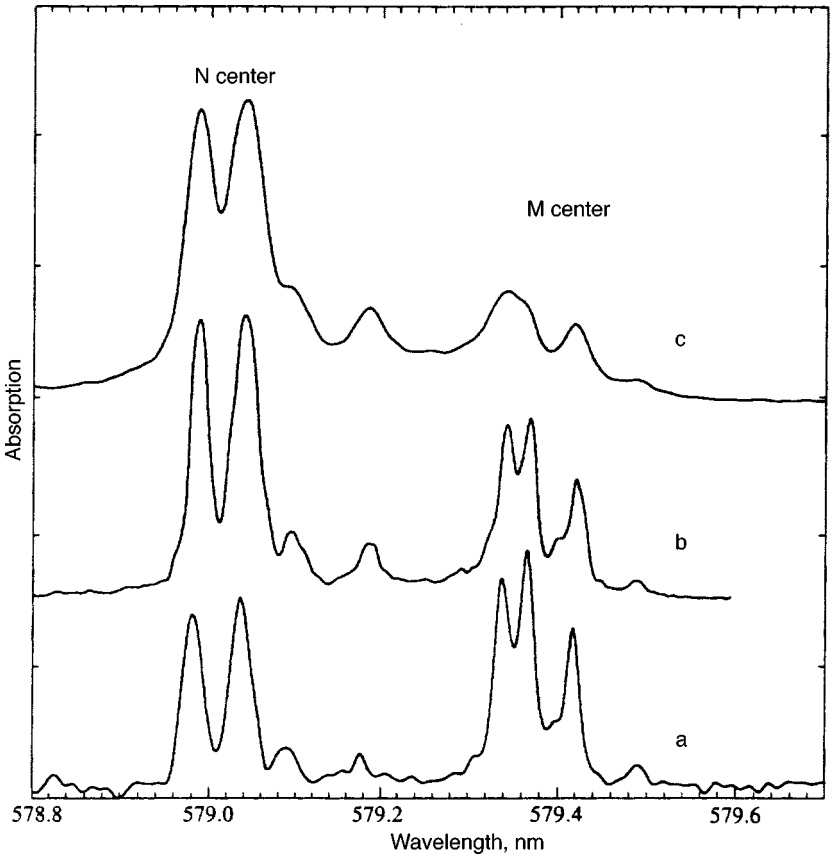

FIG. 2. Fragments of the absorption spectra of the M and N Nd^{3+} centers in CaF_2 crystals in the $^4I_{9/2} \rightarrow {}^4G_{5/2}, {}^2G_{7/2}$ transition at $T=9$ K for various concentrations of NdF_3, wt. %: a) 0.1, b) 0.3, c) 1.

gests that the complex structure of each group of lines is a consequence of the splitting of the $^4G_{5/2}, {}^2G_{7/2}$ excited state of the Nd^{3+} ion in the dimeric and tetrameric cluster centers. This conclusion is supported by Ref. 6, in which splitting of the low-lying levels of the $^4G_{5/2}, {}^2G_{7/2}$ multiplet of the Nd^{3+} ions in N and M centers was observed with a magnitude of the order of $\sim 1\ \mathrm{cm}^{-1}$ (the first three sublevels for the M centers and the first two for the N centers). In Ref. 10 we showed that the splitting of the levels can be attributed to a coherent interaction of paired Nd^{3+} ions in M and N cluster centers. Figure 3 presents energy diagrams of the Stark levels of an Nd^{3+} ion, which were obtained from the absorption spectra of the crystals investigated. The positions of the levels are consistent with the data presented in Refs. 5–7.

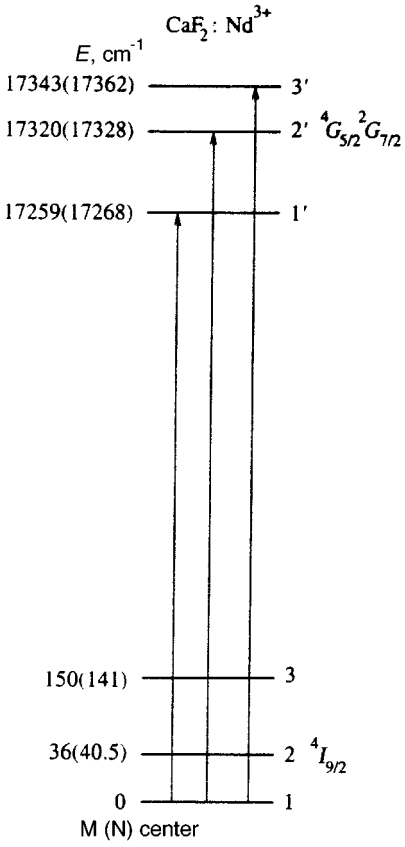

FIG. 3. Energy diagrams of the low-lying Stark levels of the $^4I_{9/2}$ and $^4G_{5/2}, {}^2G_{7/2}$ multiplets of Nd^{3+} ions in the M and N centers in a CaF_2 crystal.

3. ACCUMULATED PHOTON ECHOES IN CALCIUM FLUORIDE CRYSTALS

Accumulated photon echoes,[3,4] which are based on nonlinear resonant four-wave mixing, were used to measure the phase relaxation time T_2. The resonant excitation of Nd^{3+} ions was effected in the $^4I_{9/2} \rightarrow {}^4G_{5/2}, {}^2G_{7/2}$ transition using a Rhodamine 6G dye laser that is tunable in the range 560–600 nm. The dye laser was synchronously pumped by the second-harmonic emission ($\lambda_p = 532$ nm) of a YAG:Nd^{3+} laser operating in an active mode-locking regime with a frequency of 82 MHz. Compression of the pump laser pulses using a fiber-grating compressor was employed to shorten the duration of the output pulses of the dye laser from $\tau = 18$ to 0.5 ps. When the duration of the output pulses was $\tau = 18$ ps, the width of the spectrum of the pulses was

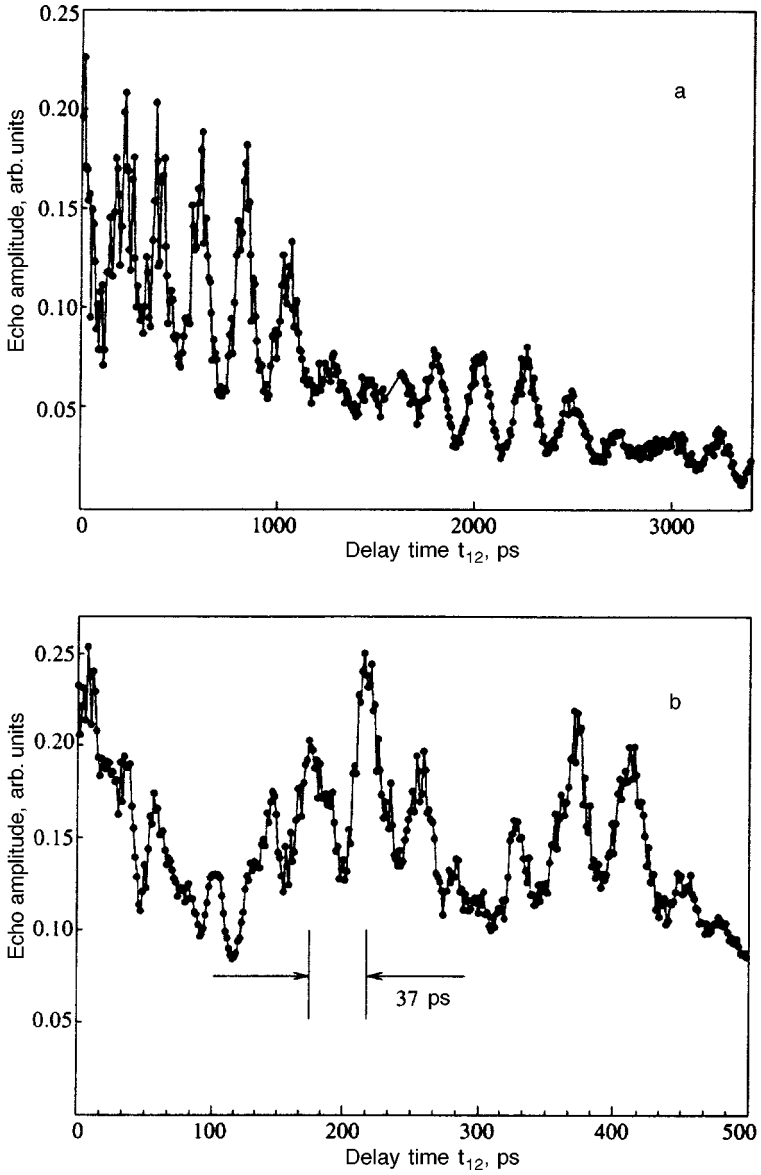

FIG. 4. Kinetics of the accumulated photon-echo signal (a) upon excitation of M centers ($\lambda = 579.36$ nm) in a CaF_2:Nd^{3+}(0.3 wt. %) crystal at $T = 9$ K; b) sample of the kinetics of accumulated photon echoes.

$\Delta\nu = 1\ \mathrm{cm}^{-1}$, and for $\tau = 0.5$ ps it was $\Delta\nu = 40\ \mathrm{cm}^{-1}$. The emission of the 20–100 mW dye laser was divided into orthogonally polarized pump beams and a probe beam in a 7:1 ratio. The probe pulses were delayed relative to the pump pulses by a time t_{12} ranging from 0 to 3.4 ns using an optical delay line. The pump beam was modulated by an acousto-optical modulator with a modulation frequency of 4 MHz. The pump beam and the probe beam then converged at a 1.5° angle and were focused onto the sample. The amplitude of the photon echo pulses was recorded in the direction of the probe beam using synchronous detection at the modulation frequency of the pump beam.

After excitation, the Nd^{3+} ions undergo rapid radiationless relaxation through several multiplets to the metastable $^4F_{3/2}$ level. The lifetime of the metastable $^4F_{3/2}$ level in the crystals investigated is long (hundreds of microseconds) in comparison with the time between pairs of exciting pulses (12 ns). This very relationship is responsible for accumulation of the echo signal. In the experiment, the amplitude of the accumulated photon-echo signal was investigated as a function of the delay between the probe pulses and pump pulses. In the experimental geometry, the echo signal decays according to $S \propto \exp(-2t_{12}/T_2)$, where t_{12} is the delay between the probe and pump pulses, and T_2 is the phase relaxation time ($T_2 = 1/(\pi\Gamma_h)$).[3]

Figure 4 presents the dependence of the accumulated photon-echo signal on the delay t_{12} for a CaF_2 crystal containing 0.3 wt. % NdF_3 at $T = 9$ K and an excitation wavelength $\lambda = 579.36$ nm. This wavelength falls between the two strongest absorption peaks assigned to the M centers (Fig. 2). As we see from the figure, the kinetics of the accumulated photon-echo signal exhibit pronounced amplitude modulation. The oscillations with a period of 37 ps correspond to the splitting between the absorption peaks of the M centers ($0.9\ \mathrm{cm}^{-1}$), which can be seen in the absorption spectrum (Fig. 2). Oscillations at a longer period correspond to smaller splitting values and cannot be seen in the absorption spectrum due to the inhomogeneous broadening of the lines and the limited spectral resolution of the monochromator. As we showed in Ref. 10, such modulation of the

TABLE I. Phase relaxation times T_2 and homogeneous linewidths $[\Gamma_h = (\pi T_2)^{-1}]$ of the ${}^4I_{9/2} \rightarrow {}^4G_{5/2}$, ${}^2G_{7/2}$ transitions of Nd^{3+} ions in the M and N centers in a CaF_2 crystal.

Transition (center)	T_2, ps	Γ_h, GHz	Wavelength, nm	T, K
$1 \rightarrow 1'(M)$	6300	0.05	579.43	9
$1 \rightarrow 1'(M)$	1200	0.27	579.43	18
$1 \rightarrow 1'(N)$	3500	0.09	579.09	9
$1 \rightarrow 1'(N)$	1000	0.32	579.09	18
$1 \rightarrow 2'(M)$	110	3.0	577.29	9
$1 \rightarrow 2'(N)$	150	2.1	577.00	9
$1 \rightarrow 3'(M)$	45	7.0	576.54	9
$1 \rightarrow 3'(N)$	30	10	575.91	9

accumulated photon-echo signal is due to fine splitting ($0.1-1\ cm^{-1}$) of the ground ${}^4I_{9/2}$ and excited ${}^4G_{5/2}, {}^2G_{7/2}$ multiplets as a result of the coherent exchange, magnetic dipole–dipole, and electric quadrupole–quadrupole interactions of the Nd^{3+} ions in the dimeric M and tetrameric N centers. The beat contrast in the kinetics depended on the excitation wavelength and decreased with increasing temperature or increasing concentration of the Nd^{3+} ions. At the same time, no variation of the decay time of the accumulated photon-echo signal was noted in the present experiments (for concentrations of NdF_3 equal to 0.3 and 1.0 wt. %). The decrease in the oscillation amplitude as the impurity-ion concentration increases might result from variation of the fine splittings in the centers that emerges as the inhomogeneous linewidth increases. Variation of the splittings leads to variation of the oscillation periods and, as a result of averaging, to a decrease in the oscillation amplitude. In addition, as can be seen from Fig. 4, the high-frequency modulation depth decreased as the delay t_{12} increased.

The echo kinetics measured in the experiment at $T=9$ K were not exponential. The reasons for this nonexponential behavior were discussed in Refs. 11 and 12, and might be associated with saturation effects at high laser pump power, as well as with the simultaneous excitation of several optical centers having different values of T_2. To minimize the influence of saturation effects, we selected a low radiated pump power of ~ 20 mW. In particular, we controlled and monitored the excitation selectivity of the centers and the transitions by varying the width of the laser excitation spectrum.

The influence of the optical density can also lead to distortion of the initial stage of decay of accumulated photon echoes.[13] It is difficult to determine the optical density of CaF_2 crystals, since the spectral width of the absorption line at $T=9$ K (Fig. 1) is less than the spectral resolution of the monochromator. Taking into account all the facts just cited, we measured the dephasing time T_2 in the final stage of decay of the accumulated photon-echo signal. In addition, to minimize the influence of oscillations and reduce the influence of optical density, the M and N centers were excited at the edge of the absorption band of each center (Fig. 2).

Table I lists T_2 and the linewidth Γ_h for transitions from the ground-state ${}^4I_{9/2}$ multiplet to the low-lying Stark sublevels of the ${}^4G_{5/2}, {}^2G_{7/2}$ multiplet. As can be seen from the table, there is a sharp increase in linewidth in the transitions to the high-lying Stark sublevels. For example, the linewidth of the transition to the third Stark sublevel (7 GHz for the M centers) is more than two orders of magnitude greater than the width of the line corresponding to the transition between the low-lying Stark sublevels (0.05 GHz for the M centers). In addition, a slight difference is observed between the values of Γ_h for the N and M centers.

The dependence of the decay time of the kinetics of the ${}^4I_{9/2} \rightarrow {}^4G_{5/2}, {}^2G_{7/2}$ transition between the low-lying Stark levels in a CaF_2:Nd^{3+} crystal was investigated in this work in the temperature range 9–50 K. Figures 5 and 6 show the experimental kinetics of the accumulated photon echoes for the excitation of M and N centers in a CaF_2 crystal (with excitation wavelengths $\lambda = 579.09$ nm and $\lambda = 579.43$ nm for the N and M centers, respectively) with a concentration of NdF_3 equal to 0.3 wt. % at $T=9$ (a) and 18 K (b). Measurements of the dephasing time and the values of the homogeneous width of the spectrum calculated from them are presented as a function of temperature for the N and M centers in CaF_2 in Fig. 7. As is seen from the figure, the widths of the N and M lines are similar over the measured temperature range, and increase monotonically with increasing temperature. At the same time, it should be noted that at $T=10$ K, the homogeneous linewidth Γ_h for the ${}^4I_{9/2} \rightarrow {}^4G_{5/2}, {}^2G_{7/2}$ transition of Nd^{3+} ions in CaF_2 crystals ($\Gamma_h \sim 0.05$ GHz) is almost an order of magnitude less than Γ_h in the disordered CaF_2–YF_3:Nd^{3+} crystals ($\Gamma_h \sim 0.05$ GHz) that we investigated in Ref. 12.

4. MECHANISM OF OPTICAL DEPHASING IN CALCIUM FLUORIDE CRYSTALS

To ascertain the mechanism of optical dephasing in these media, we analyzed the temperature dependence of the homogeneous linewidth (Fig. 7) in direct relaxational transitions between Stark sublevels involving the resonant absorption and emission of one phonon. In this approximation, the equation for the homogeneous linewidth $\Gamma_{11'}$ of the ${}^4I_{9/2} \rightarrow {}^4G_{5/2}, {}^2G_{7/2}$ transition between the low-lying Stark levels of the ground and excited multiplets (Fig. 6) can be written in the form[14]

$$\Gamma_{11'} = \frac{W_{12}^0}{\exp(\Delta E_{12}/kT)-1} + \frac{W_{13}^0}{\exp(\Delta E_{13}/kT)-1} + \frac{W_{1'2'}^0}{\exp(\Delta E_{1'2'}/kT)-1} + \frac{W_{1'3'}^0}{\exp(\Delta E_{1'3'}/kT)-1} + \frac{1}{2\pi T_1}, \quad (1)$$

where W_{12}^0, W_{13}^0, $W_{1'2'}^0$, and $W_{1'3'}^0$ are amplitude parameters that characterize the rates of radiationless relaxation between levels 1 and 2 and between levels 1 and 3 of the ground ${}^4I_{9/2}$ multiplet and between levels $1'$ and $2'$ and between levels $1'$ and $3'$ of the excited ${}^4G_{5/2}, {}^2G_{7/2}$ multiplet; ΔE_{ij} is the energy gap between the corresponding Stark sublevels (Fig. 3); and T_1 is the relaxation time of the population of the excited level. It was shown in Ref. 15 that the

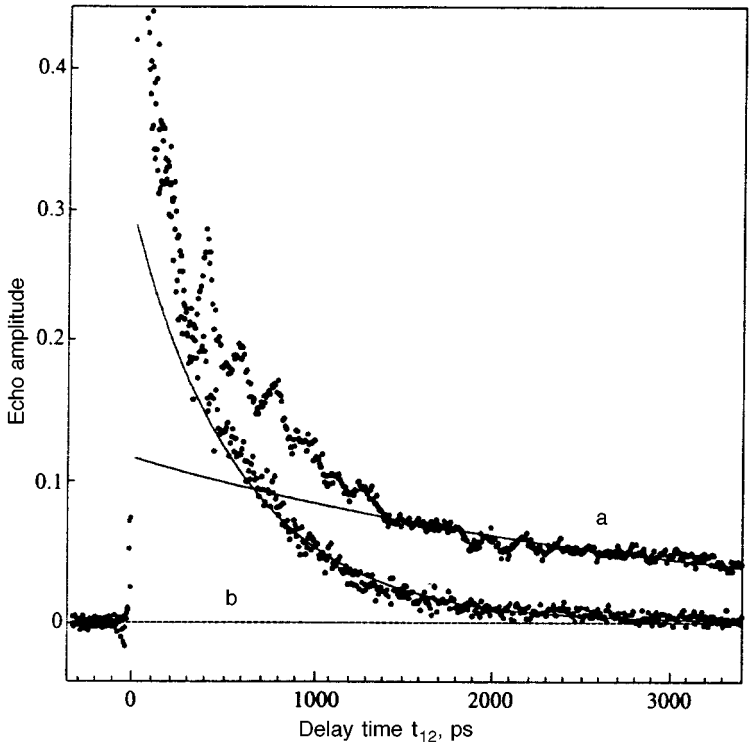

FIG. 5. Kinetics of the accumulated photon-echo signal upon excitation of the M centers ($\lambda = 579.43$ nm) in a CaF_2:Nd^{3+}(0.3 wt. %) crystal at $T = 9$ K (a) and $T = 18$ K (b). The solid lines correspond to exponential decay of the accumulated photon-echo signal; $T_2 = 6.3$ ns (a) and $T_2 = 1.2$ ns (b).

multiphonon relaxation rate $(2\pi T_1)^{-1}$ varies only slightly between liquid helium and liquid nitrogen temperatures. For this reason, we assume that the multiphonon relaxation rate $(2\pi T_1)^{-1}$ is the same for the first three Stark sublevels of the $^4G_{5/2}$,$^2G_{7/2}$ multiplet. Thus, in Eq. (1) the temperature-dependent terms describe only processes involving the absorption of a phonon.

We confined ourselves to transitions between three low-lying Stark sublevels, whose transition rates can dominate the relaxation process at $T < 50$ K. In analyzing Eq. (1) we also neglected transitions within the system of the fine-structure splitting of the M and N centers with $\Delta E < 1$ cm^{-1}, since the phonon density of states at energies $h\nu = \Delta E < 1$ cm^{-1} is low. While we only consider processes

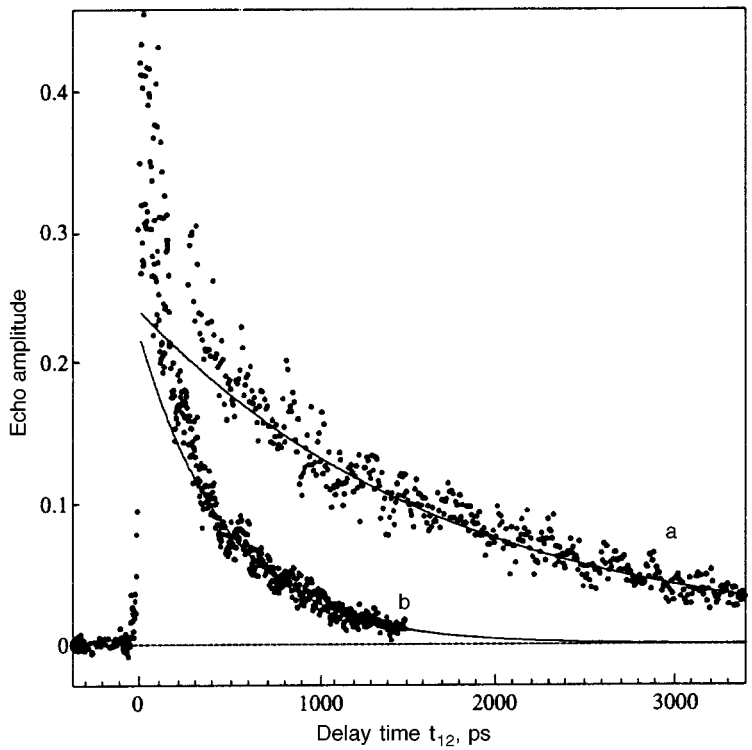

FIG. 6. Kinetics of the accumulated photon-echo signal upon excitation of the N centers ($\lambda = 579.09$ nm) in a CaF_2:Nd^{3+}(0.3 wt. %) crystal at $T = 9$ K (a) and $T = 18$ K (b). The solid lines correspond to exponential decay of the accumulated photon-echo signal; $T_2 = 3.5$ ns (a) and $T_2 = 1.0$ ns (b).

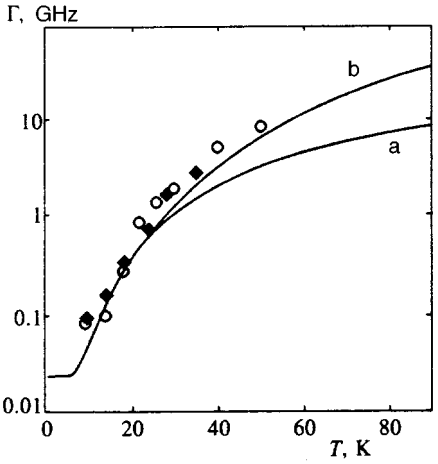

FIG. 7. Temperature dependence of the homogeneous linewidth Γ_h of the ${}^4I_{9/2}\rightarrow{}^4G_{5/2},{}^2G_{7/2}$ transition between low-lying Stark sublevels of the *M* and *N* Nd^{3+} centers (○ and ◆, respectively) in a CaF_2 crystal. The solid curves are theoretical plots obtained without (a) and with (b) consideration of W_{13}^0.

involving the absorption of a single phonon when a low-lying Stark sublevel of the ${}^4G_{5/2},{}^2G_{7/2}$ state is excited, we should take processes that entail phonon emission when high-lying Stark sublevels of this compound are excited into account. For example, for the $1\rightarrow 2'$ transition to the second Stark component, we can write

$$\Gamma_{12'}=\frac{W_{12}^0}{\exp(\Delta E_{12}/kT)-1}+\frac{W_{13}^0}{\exp(\Delta E_{13}/kT)-1}+\frac{W_{2'1'}^0\exp(\Delta E_{1'2'}/kT)}{\exp(\Delta E_{1'2'}/kT)-1}+\frac{W_{2'3'}^0}{\exp(\Delta E_{2'3'}/kT)-1}+\frac{1}{2\pi T_1}. \quad (2)$$

Here, along with terms that describe processes involving the absorption of a single phonon, the third term describes the spontaneous and stimulated emission of one phonon in the $2'-1'$ transition. The expression for the homogeneous linewidth $\Gamma_{13'}$ upon excitation of the third Stark component (the $1'-3'$ transition, Fig. 3) has the form

$$\Gamma_{13'}=\frac{W_{12}^0}{\exp(\Delta E_{12}/kT)-1}+\frac{W_{13}^0}{\exp(\Delta E_{13}/kT)-1}+\frac{W_{3'1'}^0\exp(\Delta E_{1'3'}/kT)}{\exp(\Delta E_{1'3'}/kT)-1}+\frac{W_{3'2'}^0\exp(\Delta E_{2'3'}/kT)}{\exp(\Delta E_{2'3'}/kT)-1}+\frac{1}{2\pi T_1}. \quad (3)$$

In Eqs. (1), (2), and (3), the energy gaps and the amplitude terms are symmetric under interchange of the level indices: $W_{ij}=W_{ji}$. This greatly simplifies the solution of the problem. Because of the exponentially small term $1/[\exp(\Delta E/kT)-1]$ at $T=9$ K ($kT=6.3$ cm^{-1}), Eqs. (2) and (3) can be simplified for Stark splittings $\Delta E>30$ cm^{-1} (Fig. 3). In particular, all terms except the third in (2) and the third and fourth in (3) can be neglected. In this approximation, $\Gamma_{12'}$ is equal to $W_{1'2'}^0$, since the ratio between the exponential terms in the third term in (2) for $T=9$ K and the energy gaps given is 1.

Hence, using the data in Table I, we at once obtain the radiationless relaxation constants $W_{1'2'}^0=3$ GHz (for the *M* centers) and $W_{1'2'}^0=2.1$ GHz (for the *N* centers). For this same reason, from (3) we obtain the expression $\Gamma_{13'}=W_{3'1'}^0+W_{3'2'}^0$. For subsequent evaluations we need the relationship between $W_{3'1'}^0$ and $W_{3'2'}^0$. According to the theory of electron–phonon interactions, W_{ij} is proportional to the product of the square of the matrix element of the electron–phonon interaction and the spectral phonon density of states. In the Debye approximation, the latter is proportional to the cube of the frequency of the phonon participating in the interaction. On this basis we can estimate the ratio $W_{3'2'}^0/W_{3'1'}^0=(\Delta E_{2'3'}/\Delta E_{1'3'})^3$, which is equal to 0.02 and 0.06 for the *M* and *N* centers, respectively. As a result of the evaluations made, in (3) we can neglect the term containing $W_{3'2'}^0$ and determine the constants $W_{3'1'}^0=\Gamma_{13'}$, which are 7 and 10 GHz for the *M* and *N* centers, respectively. The ratios between the resulting values are $W_{3'1'}^0/W_{2'1'}^0=2.3$ (4.3) for the *M* (*N*) centers. A comparison of these ratios with the ratio $(\Delta E_{3'1'}/\Delta E_{2'1'})^3=2.7$ (4.3) exhibits good agreement with the Debye approximation.

The significant difference between ΔE_{12} (~ 35 cm^{-1}) and ΔE_{13} (~ 150 cm^{-1}) for the ground-state ${}^4I_{9/2}$ multiplet causes the second term in (1) to be negligible in comparison with the first at $T<20$ K. It should be noted that the determination of W_{12}^0 from (1) at $T=9$ K is very sensitive to the accuracy of the measurements. First, the maximum delay between the pump pulses and probe pulses in the experimental system is $t_{12}=3.4$ ns, and this complicates the determination of a damping decrement of an accumulated photon-echo signal that is comparable to this time. Second, the values of T_1 obtained in Ref. 16 were 7.2 ns and 3.3 ns for the *M* and *N* centers in a CaF_2:Nd^{3+} crystal, respectively; therefore, a difference between two similar values (for example, $T_1(M)=7.2$ ns and $T_2(M)=6.3$ ns, see Table I) must be taken to calculate $W_{12}^0\sim(\Gamma_{11'}-(2\pi T_1)^{-1})$. Consequently, we used the results of kinetic measurements of the decay of the accumulated photon-echo signal at $T=18$ K, where $T_2(M)=1.2$ ns, to calculate W_{12}^0. The value of $\Gamma_{11'}$ in these experiments was 0.27 (0.30 GHz) for the *M* (*N*) centers. As a result, W_{12}^0 calculated from Eq. (1) was 3.4 and 5.9 GHz for the *M* and *N* centers, respectively.

In Fig. 7 (curve a) the solid line shows the dependence of $\Gamma(T)$ obtained from Eq. (1) for the *M* centers in a CaF_2:Nd^{3+} crystal with exact consideration of the transitions to the second and third Stark levels of the excited state and to the second level of the ground state, but without considering the relaxation processes associated with phonon absorption between levels 1 and 3 of the ground state ($W_{13}^0=0$). The figure reveals a sharp increase in the difference between the experimental points and the theoretical curve at $T>30$ K. This difference may be associated with neglect of relaxation processes between levels 1 and 3 of the ground state, which

becomes unjustified as the temperature rises. In order to take these processes into account, we determined W_{13}^0 by assuming that the phonon density of states has a Debye distribution. This assumption enables us to determine the relationship between W_{13}^0 and W_{12}^0 as $W_{13}^0 = W_{12}^0(\Delta E_{13}/\Delta E_{12})^3$ ($W_{13}^0 = 260$ (270) GHz for the M (N) centers). A theoretical curve that takes these parameters into account is depicted in Fig. 7 (curve b). The experimental values clearly correspond to a direct relaxational dephasing process in the temperature range considered.

Thus, the mechanism of optical dephasing in multicenter ordered crystals over the range $T = 10-50$ K is described well by a single-phonon resonant relaxation process. We previously showed that the temperature dependence of optical dephasing in disordered CaF_2-YF_3 crystals is also described by single-phonon processes.[12] The tenfold difference between the relaxation rate in disordered CaF_2-YF_3(10%):Nd^{3+} crystals with $\Gamma_h = 0.5$ GHz and in ordered CaF_2:Nd^{3+} crystals ($\Gamma_h = 0.05$ GHz) at $T = 9$ K can be associated with the difference between the probabilities W_{ij}^0 (Eq. (1)). In Ref. 17 we measured the absorption spectra of these crystals in the far infrared ($10-100\ \mathrm{cm}^{-1}$), and showed that the absorption coefficient in the frequency range corresponding to direct single-phonon transitions ($10-100\ \mathrm{cm}^{-1}$) increases by about an order of magnitude upon passage from an ordered crystal of fluorite, CaF_2, to disordered crystals of yttrofluorite, CaF_2-YF_3(12 wt. %). Assuming that there is a correlation between the IR absorption coefficient and the density of the phonon states participating in direct single-phonon transitions (which was previously demonstrated for amorphous semiconductors[18]), we can thus explain the indicated difference between the values of the probabilities W_{ij}^0, and therefore between Γ_h and the relaxation rates in ordered and disordered media.

5. CONCLUSIONS

Picosecond accumulated photon echoes have been used to investigate the temperature dependence of the homogeneous width of the spectrum of the $^4I_{9/2} \rightarrow {}^4G_{5/2}, {}^2G_{7/2}$ transition of Nd^{3+} ions in ordered CaF_2 crystals in the range 9–50 K with selective excitation of rhombic M and N centers. The homogeneous linewidths of the transitions between the low-lying Stark level of the ground $^4I_{9/2}$ multiplet and three levels of the excited $^4G_{5/2}, {}^2G_{7/2}$ multiplet have been measured, permitting calculation of the force constants of the relaxational single-phonon inter-Stark transitions in the ground and excited multiplets. An analysis of temperature dependence has shown that optical dephasing in the ground and excited states of the ordered crystals investigated is described well by direct relaxation processes that involve resonant inter-Stark absorption of one phonon. At $T = 9$ K, the homogeneous linewidth Γ_h in the disordered crystals is almost an order of magnitude greater than the analogous value in the ordered crystals. This difference can be accounted for by a significantly higher spectral phonon density of states in the disordered crystals.

This research was performed with support from the Russian Fund for Fundamental Research (Project 95-02-04328-a).

[1] R. M. Macfarlane and R. M. Shelby, in *Spectroscopy of Solids Containing Rare Earth Ions*, A. A. Kaplyanskii and R. M. Macfarlane (eds.), Elsevier, Amsterdam (1987), Vol. 21, p. 51.
[2] O. K. Alimov, T. T. Basiev, and S. B. Mirov, *Selective Laser Spectroscopy (Proceedings of the Institute of General Physics of the Academy of Sciences of the USSR, Vol. 9)* [in Russian], Nauka, Moscow (1987).
[3] W. H. Hesselink and D. A. Wiersma, Phys. Rev. Lett. **43**, 1991 (1979).
[4] H. de Vries and D. A. Wiersma, J. Chem. Phys. **80**, 657 (1984).
[5] Yu. K. Voron'ko, A. A. Kaminskiĭ, and V. V. Osiko, Zh. Éksp. Teor. Fiz. **49**, 420 (1965) [Sov. Phys. JETP **22**, 295 (1966)].
[6] T. P. J. Han, G. D. Jones, and R. W. Syme, Phys. Rev. B **47**, 14 706 (1993).
[7] V. V. Osiko, Yu. K. Voron'ko, and A. A. Sobol, in *Crystals: Growth, Properties and Applications, Vol. 10*, Springer-Verlag, Berlin–Heidelberg (1984), pp. 37–86.
[8] N. E. Kask, L. S. Kornienko, and E. G. Lariontsev, Fiz. Tverd. Tela (Leningrad) **8**, 2572 (1966) [Sov. Phys. Solid State **8**, 2058 (1967)].
[9] N. E. Kask, L. S. Kornienko, and M. Fakir, Fiz. Tverd. Tela (Leningrad) **6**, 549 (1964) [Sov. Phys. Solid State **6**, 430 (1964)].
[10] V. V. Fedorov, T. T. Basiev, A. Ya. Karasik *et al.*, in *Conference Handbook ICL '96*, Prague (1996), p. 12.
[11] K. W. Ver Steeg, A. Ya. Karasik, R. J. Reeves *et al.*, J. Lumin. **60/61**, 741 (1994).
[12] K. W. Ver Steeg, A. Ya. Karasik, R. J. Reeves *et al.*, Phys. Rev. B **51**, 6085 (1995).
[13] S. Saikan, H. Miyamoto, Y. Tosaki *et al.*, Phys. Rev. B **36**, 5074 (1987).
[14] *Laser Spectroscopy of Solids*, W. M. Yen and P. M. Selver (eds.), Springer-Verlag, Berlin (1981).
[15] T. T. Basiev, A. Yu. Dergachev, Yu. V. Orlovskiĭ *et al.*, in *Kinetic Laser-Fluorescence Spectroscopy of Laser Crystals* (*Proceedings of the Institute of General Physics of the Russian Academy of Sciences, Vol.* **46**) [in Russian], Nauka, Moscow (1994).
[16] Y. V. Orlovskii, S. B. Abalakin, and I. N. Vorob'ev, in *Abstracts of DPC-97: 11th International Conference on Dynamical Processes in Excited States of Solids*, Mittelberg, Austria–Germany (1997).
[17] A. Ya. Karasik, T. T. Basiev, A. A. Volkov *et al.*, in *Conference Handbook ICL '96*, Prague (1996), p. 2.
[18] *Light Scattering in Solids I (Topics in Applied Physics, Vol. 8)*, M. Cardona (ed.), Springer, Berlin (1975).

Translated by P. Shelnitz